Inorganic Chemistry

Article

pubs.acs.org/IC

Integration of Alkyl-Substituted Bipyridyl Benzenedithiolato Platinum(II) Complexes with Cadmium(II) Ion via Selective Dative Bond Formation

Hirotaka Honda,[†] Takeshi Matsumoto,[†,‡] Misaki Sakamoto,[†] Atsushi Kobayashi,[†] Ho-Chol Chang,*[,†] and Masako Kato[†,‡]

[†]Department of Chemistry, and [‡]Center for Strategic Utilization of Elements, Faculty of Science, Hokkaido University, North-10, West-8, Kita-ku, Sapporo 060-0810, Japan

Supporting Information

ABSTRACT: The presence of lone pairs on the Pt and S atoms of [Pt(Bdt)(DTBbpy)] (**1**) (Bdt = 1,2-benzenedithiolato and DTBbpy = 4,4′-di-*tert*-butyl-2,2′-bipyridine) and [Pt(Bdt)(C13bpy)] (**2**) (C13bpy = 4,4′-ditridecyl-2,2′-bipyridine) led to selective dative bond formation with Cd(II). Complexes **1** and **2** show no binding interaction with Zn(II), while they bind selectively with Cd(II) to give a twisted trinuclear complex, $[Cd\{Pt(Bdt)(DTBbpy)\}_2(ClO_4)(H_2O)](ClO_4)$ (**3**), and a shuttlecock-shaped tetranuclear complex, $[Cd\{Pt(Bdt)(C13bpy)\}_3(H_2O)](ClO_4)_2\cdot CH_2Cl_2$ (**4**), respectively, depending upon the alkyl groups substituted on the 2,2′-bipyridine. The two platinum moieties in **3** are connected to the seven-coordinated Cd atom through Pt → Cd (2.7331(7) and 2.7936(7) Å) and S → Cd (2.690(3), 2.940(3), and 3.067(3) Å) dative bonds, while the three moieties in **4** are connected to the tetrahedral Cd atom only by S → Cd (2.552(4) Å) dative bonds. These structural variations found in **3** and **4** are caused not only by steric hindrance of the *t*-Bu groups but also by the microsegregation effect derived from the tridecyl chains. The three platinum moieties in **4** align so as to form a parallel orientation of their dipole moments, in contrast to the twisted arrangement found in **3**. The dative bonds formed in **3** and **4** are commonly stable in the solid state and in less coordinative solvents such as dichloromethane, while dissociation behavior of platinum moieties with Cd(II) was observed in more coordinative THF. UV−vis and NMR spectroscopy unsealed the characteristic association/dissociation properties depending on the coordination abilities of solvents. Finally, the present study revealed that the formation of dative bonds between the platinum moieties with Cd(II) plays important roles not only in stabilizing the ground states, which leads to blue shifts in both absorption and emission energies, but also in electronic interactions between the moieties, which are revealed by electrochemical studies.

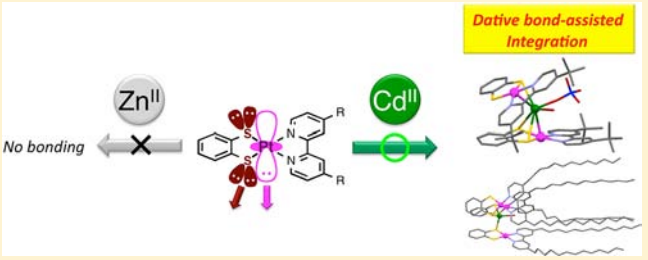

INTRODUCTION

A family of square-planar [Pt(L)(R-bpy)] complexes, where L is an anionic ligand such as Cl^-, CN^-, NCS^-, and R-bpy refers to an alkyl-substituted-2,2′-bipyridine, has been known to show not only intriguing photochemical properties, including chromic and luminescence behavior,[1] but also photosensitizing properties in photocatalytic hydrogen production reactions.[1b,2] These characteristics are inherently based on electronic interactions between a central platinum ion with a heavy metal effect and two different coordinating ligands, L- and R-bpy, for both ground states and long-lived excited states.

Scheme 1. Lone pair electrons on [Pt(Bdt)(R-bpy)]

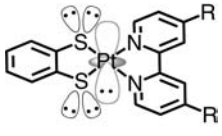

Furthermore, the physicochemical properties of these complexes have been modulated and/or improved by constructing supramolecular assemblies via intermolecular interactions: these complexes have a tendency to assemble via intermolecular Pt(II)···Pt(II) interactions,[3] dipole−dipole interactions,[4] $\pi\cdots\pi$ interactions of ligands,[3c,5] hydrogen bonding,[6] and bridging ligands such as bis(diphenylphosphino)methane.[7] The formation of supramolecular assemblies resulted in significant variations in physical properties compared with those in discrete states, for example, enhancement in luminescence intensities,[3a] variations in phase behaviors,[4] and increases in hydrogen evolution efficiency.[2a]

In addition to the aforementioned supramolecular assemblies, our group has investigated a series of platinum complexes

Received: October 29, 2012
Published: March 29, 2013

   dx.doi.org/10.1021/ic302352k | *Inorg. Chem.* 2013, 52, 4324−4334

such as [Pt(Bdt)(R-bpy)] shown in Scheme 1, where Bdt refers to redox-active 1,2-benzenedithiolato.[8a] In particular, the introduction of two 3-octyltridecyl groups on the 4,4′-positions of bpy led to the formation of a hexagonal columnar ordered liquid crystal phase constructed from dipole−dipole interactions based on the asymmetric molecular shape. These complexes show interesting integrated functions derived from thermally fluctuating structures and photochemical and redox activity on the mesogen.[8]

Here we refocused on the molecular structure of the complexes. The asymmetric molecular shape contributes to a dipole-driven self-assembly process of the complexes both in crystalline phases in [Pt(Bdt)(C13bpy)] (C13bpy = 4,4′-ditridecyl-2,2′-bipyridine)[4] and in liquid crystalline phases in [Pt(Bdt)(C8,10bpy)] (C8,10bpy = 4,4′-di(3-octyltridecyl)-2,2′-bipyridine).[8a] In contrast, lone pair electrons in a d_{z2} orbital of the Pt and on the coordinating S atoms of the Bdt remain active toward the organization of the moieties. It is noteworthy that such localized lone pairs have been known to form a dative bond with Lewis acids:[9] Yamaguchi et al. reported a Pt → Cd-type dative bond in $[\{Pt(CH_3)_2(bpy)\}\{Cd(cyclen)\}](ClO_4)_2$ (cyclen = 1,4,7,10-tetraazacyclododecane),[9a] while Chen et al. found dative bonding between the S atoms of 3,4-toluenedithiolato (tdt) with the Ag and Au atoms in $[PtAg_2(dmbpy)(tdt)(dppm)_2](SbF_6)_2$ (dmbpy = 4,4′-dimethyl-2,2′-bipyridine and dppm = bis(diphenylphosphino)-methane) and $[PtAu_2(dmbpy)(tdt)(dppm)_2](SbF_6)_2$.[9b,c] In contrast, no example has been reported on the integration of two or more [Pt(Bdt)(R-bpy)] moieties via dative bonds. The integration of such functional moieties would show facilitating assembled effects in their optoelectronic properties as a result of interactions between the moieties through dative bonds.

In this paper, we first investigated the selectivity in dative bond formation of [Pt(Bdt)(DTBbpy)] (**1**) (DTBbpy = 4,4′-di-*tert*-butyl-2,2′-bipyridine) and [Pt(Bdt)(C13bpy)] (**2**) with Zn(II) and Cd(II), which possess different softness.[10] In addition to the different nature of these two metal ions, alternative effects were expected because of the differences in the size of the *t*-Bu (**1**) and tridecyl (**2**) alkyl groups on the 4,4′-positions of bpy. They serve as important structural parameters that may alter the assembling fashions of the moieties and Lewis acid, by which their spectroscopic and redox properties would be tuned.

EXPERIMENTAL SECTION

General Procedures. 1,2-Benzenedithiol ($BdtH_2$), DTBbpy, and zinc perchlorate hexahydrate were purchased from Sigma-Aldrich Chemicals. Potassium tetrachloroplatinate(II) ($K_2[PtCl_4]$) was purchased from Furuya Metal Co., Ltd. Cadmium perchlorate hexahydrate and sodium hydroxide (NaOH) were purchased from Wako Pure Chemical Industries. C13bpy[11] and $[PtCl_2(C13bpy)]$[8b] were synthesized by the literature methods. All of the solvents for the syntheses and the measurements were distilled by standard methods under N_2 atmosphere. All synthetic operations were performed under N_2 atmosphere using Schlenk line techniques.

Syntheses. *[$PtCl_2$(DTBbpy)].*[2c] 13.5 mL of 3 M HCl and 10 mL of $CHCl_3$ were added to a mixture of $K_2[PtCl_4]$ (4.1598 g, 10.021 mmol) and DTBbpy (2.7001 g, 10.060 mmol). The mixture was heated at 95 °C for 24 h to afford a yellow precipitate. The product was filtered and washed with H_2O, MeOH, and *n*-hexane. Yield 5.1722 g (9.6787 mmol, 96.6%) FAB-MS: m/z = 534 $[M + H]^+$. ^1H NMR ($CDCl_3$, 270 MHz): δ = 9.53 (d, 2H, J = 6.3 Hz), 7.87 (d, 2H, J = 2.0 Hz), 7.50 (dd, 2H, J = 6.3, 2.0 Hz), 1.46 (s, 18H). Calcd. for $C_{18}H_{24}Cl_2N_2Pt$: C, 40.46; H, 4.53; N, 5.24. Found: C, 40.31; H, 4.34; N, 5.07.

Table 1. Crystallographic Data for 3 and 4

	3	4
formula	$C_{48}H_{58}CdCl_2N_4O_9Pt_2S_4$	$C_{126}H_{194}CdCl_2N_6O_9Pt_3S_6$
fw	1536.74	2897.90
crystal size (mm^3)	0.37 × 0.13 × 0.08	0.20 × 0.20 × 0.20
crystal system	triclinic	trigonal
space group	$P\bar{1}$ (No. 2)	$R\bar{3}$ (No. 148)
a (Å)	12.791(2)	17.1836(9)
b (Å)	14.991(2)	17.1836 (9)
c (Å)	15.375(2)	83.273(6)
α (°)	104.643 (2)	90
β (°)	91.6930(13)	90
γ (°)	107.7570(13)	120
V (Å^3)	2698.0(6)	21294(0.2)
T (K)	223	213
Z	2	6
D_{calc} (g cm^{-3})	1.891	1.356
$F(000)$	1496	8856
μ(Mo Kα) (cm^{-1})	58.523	32.598
measured reflns	21890	15609
unique reflns	11779	8046
refined parameters	631	466
GOF on F^2	1.094	1.041
R_{int}	0.0465	0.0856
$R_1{}^a$	0.0516	0.0861
$wR_2{}^b$ (all data)	0.1528	0.2754

$^aR_1 = \Sigma||F_o| - |F_c||/\Sigma|F_o|$. $^bwR_2 = \{[\Sigma w(F_o^2 - F_c^2)^2]/[\Sigma w(F_o^2)^2]\}^{1/2}$.

*[Pt(Bdt)(DTBbpy)] (**1**).*[2c] $BdtH_2$ (169.5 mg, 1.192 mmol), NaOH (126.5 mg, 3.163 mmol), and $[PtCl_2(DTBbpy)]$ (568.8 mg, 1.064 mmol) were combined in a mixed solvent of THF (60 mL) and MeOH (20 mL). The mixture was stirred at room temperature for 5 h, producing a deep-violet solution. After evaporation of the solvent, the product was washed with H_2O and dissolved in 10 mL of CH_2Cl_2 and then filtered. Addition of 40 mL of *n*-hexane afforded a reddish-violet precipitate. Removal of the solvent yielded a reddish-violet solid. Yield 535.8 mg (0.8875 mmol, 83.4%). FAB-MS: m/z = 603 $[M]^+$. ^1H NMR (CD_2Cl_2, 270 MHz): δ = 9.07 (d, 2H, J = 5.9 Hz), 7.93 (d, 2H, J = 2.0 Hz), 7.46 (dd, 2H, J = 5.9, 2.0 Hz), 7.24 (m, 2H), 6.66 (m, 2H), 1.36 (s, 18H). Calcd. for $C_{24}H_{28}N_2PtS_2$: C, 47.75; H, 4.67; N, 4.64. Found: C, 47.61; H, 4.65; N, 4.66.

*[Pt(Bdt)(C13bpy)] (**2**).*[4] 80 mL of CH_2Cl_2 and 20 mL of MeOH were added to a mixture of $BdtH_2$ (0.3425 g, 2.409 mmol), NaOH (0.1956 g, 4.890 mmol), and $[PtCl_2(C13bpy)]$ (1.795 g, 2.281 mmol). The mixture was heated at 80 °C for 24 h, affording a deep-violet solution. After evaporation of the solvent, the product was dissolved in 45 mL of CH_2Cl_2 and filtered. Addition of 200 mL of *n*-hexane afforded a reddish-violet precipitate. Removal of the solvent yielded a reddish-violet solid. Yield 1.121 g (1.309 mmol, 57.4%). FAB-MS: m/z = 856 $[M + H]^+$. ^1H NMR (CD_2Cl_2, 270 MHz): δ = 8.94 (d, 2H, J = 5.9 Hz), 7.77 (d, 2H, J = 1.4 Hz), 7.24 (m, 4H), 6.67 (dd, 2H, J = 6.0, 3.3 Hz), 2.65 (t, 4H, J = 7.7 Hz), 1.64 (m, 4H), 1.19 (m, 40H), 0.80 (t, 6H, J = 6.6 Hz). Calcd. for $C_{42}H_{64}N_2PtS_2$: C, 58.92; H, 7.53; N, 3.27. Found: C, 58.78; H, 7.55; N, 3.30.

*[Cd{Pt(Bdt)(DTBbpy)}$_2$(ClO_4)(H_2O)](ClO_4) (**3**).* Twenty milliliters of CH_2Cl_2 and 5 mL of acetone were added to a mixture of $Cd(ClO_4)_2{\cdot}6H_2O$ (119.03 mg, 0.28381 mmol) and **1** (339.9 mg, 0.5630 mmol). The mixture was stirred at room temperature for 30 min, affording a red solution. After evaporation of the solvent, the product was dissolved in 20 mL of CH_2Cl_2 and filtered. Recrystallization from CH_2Cl_2/benzene led to the formation of orange-colored single crystals of **3**. Yield 260.85 mg (0.16974 mmol, 60.3%). FAB-MS: m/z = 1419 [**3**-H_2O-ClO_4]$^+$. ^1H NMR (CD_2Cl_2, 270 MHz): δ = 9.01 (d, 4H, J = 8.1 Hz), 8.69 (d, 4H, J = 2.7 Hz), 7.87 (dd, 4H, J = 8.1, 2.7 Hz), 7.24 (br, 4H), 6.76 (br, 4H), 1.47 (s, 36H).

dx.doi.org/10.1021/ic302352k | Inorg. Chem. 2013, 52, 4324−4334

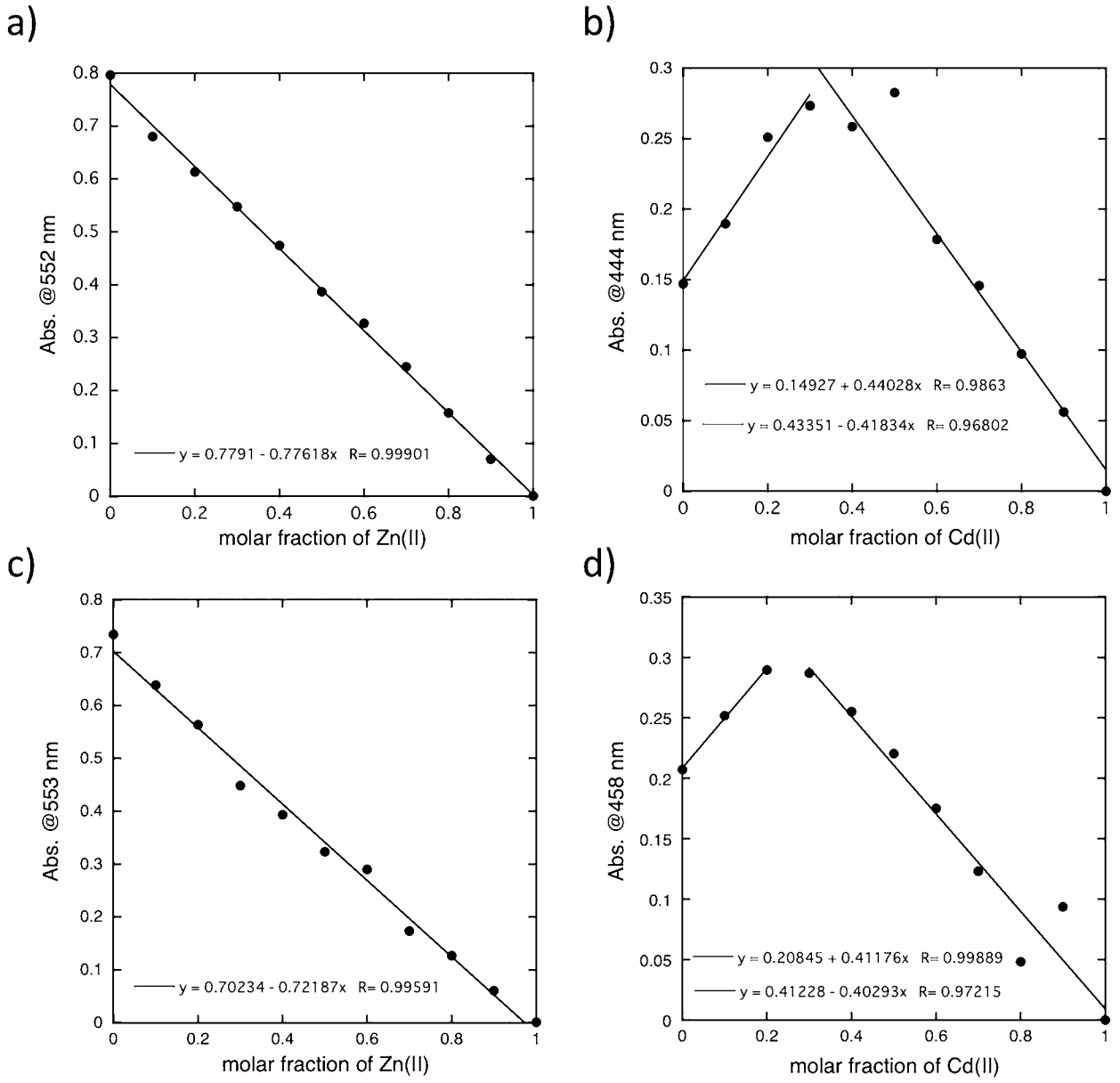

Figure 1. Job plots for **1** with (a) Zn(II) and (b) Cd(II), and those for **2** with (c) Zn(II) and (d) Cd(II) in CH_2Cl_2/acetone solutions (9:1, v/v).

Calcd. for $C_{48}H_{58}CdCl_2N_4O_9Pt_2S_4$: C, 37.52; H, 3.80; N, 3.65. Found: C, 37.42; H, 3.79; N, 3.52.

[Cd{Pt(Bdt)(C13bpy)}$_3$(H$_2$O)](ClO$_4$)$_2$·CH$_2$Cl$_2$ (**4**). Ten milliliters of CH_2Cl_2 and 3 mL of acetone were added to a mixture of $Cd(ClO_4)_2·6H_2O$ (9.064 mg, 0.02161 mmol) and **2** (47.85 mg, 0.05589 mmol). The mixture was stirred at room temperature for 30 min, affording a red solution. After evaporation of the solvent, the product was dissolved in 8.5 mL of CH_2Cl_2 and filtered. Addition of 30 mL of *n*-hexane afforded orange precipitate. Recrystallization from CH_2Cl_2/*n*-hexane led to the formation of orange-colored single crystals of **4**. Yield 45.36 mg (0.01503 mmol, 81.6%). ^{1}H NMR (CD_2Cl_2, 270 MHz): δ = 8.54 (d, 6H, J = 5.8 Hz), 7.84 (s, 6H), 7.23 (d, 6H, J = 5.8 Hz), 6.98 (dd, 6H, J = 6.1, 3.1 Hz), 6.74 (dd, 6H, J = 6.1, 3.1 Hz), 2.66 (t, 12H, J = 7.6 Hz), 1.60 (m, 6H), 1.19 (m, 126H), 0.80 (m, 18H). Calcd. for $C_{127}H_{196}CdCl_4N_6O_9Pt_3S_6$: C, 51.14; H, 6.62; N, 2.82. Found: C, 51.12; H, 6.57; N, 2.83.

Physical Measurements. ^{1}H NMR spectroscopy was performed using a JEOL EX-270 spectrometer. Elemental analyses and mass spectra were measured at the analysis center in Hokkaido University. Microphotographs were taken using an Olympus BX51 with a DP70 digital camera. Electrochemical measurements were carried out with an ALS model 650A electrochemical analyzer. A standard three-electrode system (a glassy carbon working electrode, platinum-wire counter electrode, and Ag/Ag$^+$/CH$_3$CN electrode as reference) was used in solution. Absorption spectra of the solid and solution were measured using a Hitachi U-4100 spectrophotometer. Emission spectra in the solid at 77 K were obtained using a JASCO FP-6600 spectrometer under N_2 atmosphere with a quartz cell. For emission spectra in the solid states at 77 K, the samples were fixed to the inside of a quartz cell using grease and cooled with liquid N_2 in a dewar. Emission quantum yields were measured on a Hamamatsu C9920-01 system. Emission spectra in degassed CH_2Cl_2 at 77 K were collected with a JASCO FP-6600 spectrometer under N_2 atmosphere using a quartz tube. The IR spectra were recorded on a Nicolet 6700 ET-IR spectrometer equipped with a Smart-Orbit (Diamond) ATR accessory.

Crystallographic Data Collection and Refinement of Structures. The crystallographic measurements were performed using a Rigaku AFC-7R diffractometer with a Mercury CCD area detector and graphite monochromated Mo Kα radiation (λ = 0.71069 Å). Specimens of suitable size and quality were selected and mounted on a loop. The structures were solved by direct methods (SIR2004)[12] and expanded using Fourier techniques (DIRDIF99),[13] which

dx.doi.org/10.1021/ic302352k | Inorg. Chem. 2013, 52, 4324−4334

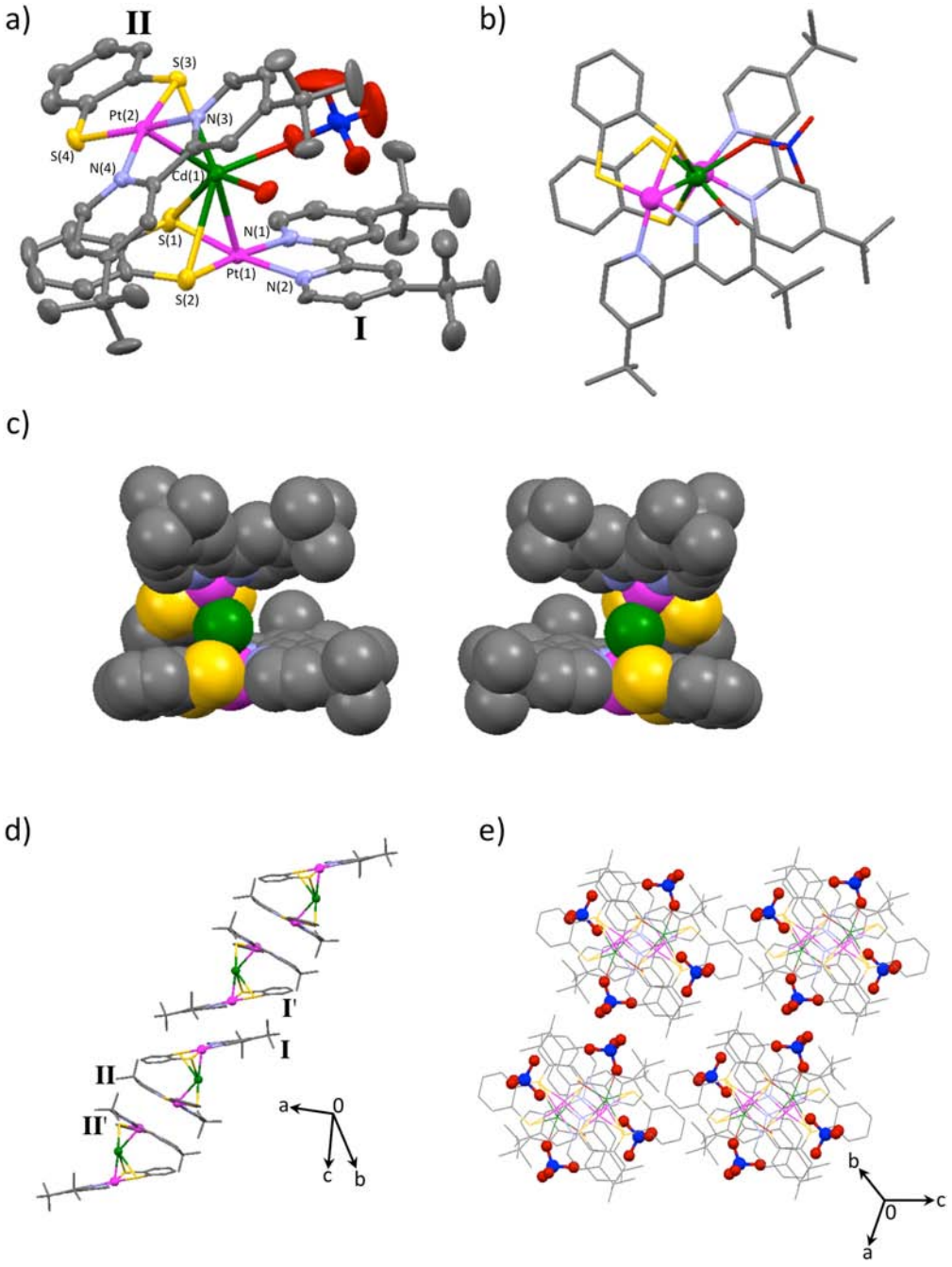

Figure 2. (a) Side (ellipsoid at 50% probability) and (b) top views of the trinuclear cation in **3** for Cd (green), Pt (magenta), S (yellow), N (blue-purple), O (red), Cl (blue), and C (gray). (c) Representation of two twisted-chiral enantiomers (water and perchlorate anion are omitted), and (d) the columnar structure of the cations in **3**. (e) View of the packing structure of **3** along the column.

successfully located non-hydrogen atoms. All calculations were performed using the CrystalStructure crystallographic software package[14] except for refinement, which was performed using SHELXL-97.[15] The crystallographic data for **3** and **4** are summarized in Table 1. Several X-ray diffraction experiments for **4** suggested two ClO_4^- counteranions being heavily disordered. Therefore, all two ClO_4^- were refined by disordered model and all O atoms of ClO_4^- were refined isotropically. Solvated CH_2Cl_2 molecule could not be refined because of the limited quality of the data set and the large unit cell parameters together with lability of the solvated CH_2Cl_2 molecules. On the other hand, the elemental analysis and IR spectrum of **4** strongly support the presence of ClO_4^- counteranions, which is consistent with the above formula (see the Supporting Information (SI)). For **4**, it was found that there are heavy disorders especially for C(32)−C(34). Full crystallographic details have been deposited with the Cambridge Crystallographic Data Centre. CCDC-907568 for **3** and CCDC-927566 for **4**.

RESULTS AND DISCUSSION

Selective Binding Behaviors of [Pt(Bdt)(R-bpy)] with Lewis Acids. The selectivity in the binding behaviors of [Pt(Bdt)(R-bpy)] (**1** and **2**) with Lewis acids and the stoichiometry of the resulting complexes were determined by Job plots. Stock CH_2Cl_2:acetone solutions (9:1, v/v) of **1** and **2** and each Lewis acid ($Zn(ClO_4)_2{\cdot}6H_2O$ and $Cd(ClO_4)_2{\cdot}6H_2O$) were prepared. In 11 separate cells, portions of the two solutions were added such that their ratio changed from 0 to 1

dx.doi.org/10.1021/ic302352k | Inorg. Chem. 2013, 52, 4324−4334

Table 2. Selected Bond Distances (Å), Angles (°), and Dihedral Angles (°) of 3 and 4

	3	4
Pt(1)−S(1)	2.261(4)	2.258(3)
Pt(1)−S(2)	2.266(3)	2.252(4)
Pt(1)−N(1)	2.054(7)	2.081(10)
Pt(1)−N(2)	2.057(8)	2.036(9)
Pt(2)−S(3)	2.271(3)	
Pt(2)−S(4)	2.244(4)	
Pt(2)−N(3)	2.054(9)	
Pt(2)−N(4)	2.051(7)	
Cd(1)−Pt(1)	2.7331(7)	
Cd(1)−Pt(2)	2.7936(7)	
Cd(1)−S(1)	3.067(3)	2.552(4)
Cd(1)−S(2)	2.940(3)	
Cd(1)−S(3)	2.690(3)	
Cd(1)−O(1)	2.286(8)	2.289(12)
Cd(1)−O(2)	2.446(9)	
S(1)−Pt(1)−S(2)	88.15(10)	89.52(11)
N(1)−Pt(1)−N(2)	78.3(3)	79.8(4)
S(1)−Pt(1)−Cd(1)	75.12(7)	
S(2)−Pt(1)−Cd(1)	71.35(6)	
Pt(1)−S(1)−Cd(1)	59.45(6)	88.20(12)
Pt(1)−S(2)−Cd(1)	61.74(6)	
S(3)−Pt(2)−S(4)	89.15(10)	
N(3)−Pt(2)−N(4)	78.7(4)	
S(3)−Pt(2)−Cd(1)	63.19(6)	
S(4)−Pt(2)−Cd(1)	99.31(7)	
Pt(2)−S(3)−Cd(1)	67.93(7)	
Bdt(**I**, C_6S_2)/Pt(1)N(1)N(2)S(1)S(2)	12.34	8.15
Bdt(**II**, C_6S_2)/Pt(2)N(3)N(4)S(3)S(4)	4.73	

while maintaining a total volume of 4 mL. Experimental Job plots for different total concentrations of **1** and **2** and both Lewis acids are shown in Figure 1. The absorbances of **1** or **2** with Zn(II) decrease linearly, indicating that neither complex has an interaction with Zn(II) (Figure 1a,c). However, in the case of titration of **1** with Cd(II), the Job plot shows a maximum value for the absorbance at 444 nm when the mole fraction of Cd(II) reaches 0.33, which is a signature of a 1:2 binding between Cd(II) and **1** (Figure 1b). In contrast, in the case of **2**, the Job plot demonstrates a maximum value for the absorbance at 458 nm when the mole fraction of Cd(II) reaches to 0.25, which is a signature of a 1:3 binding between Cd(II) and **2** (Figure 1d). As seen above, the selective binding of the Lewis acid is clear from the Job plots, which also reveals that the bindings depend not only on the Lewis acids but also on the alkyl substituents of the R-bpy. The observed selectivity in binding behaviors can be rationalized in terms of the differences in softness of Zn(II) and Cd(II).[10]

Molecular Structures of 3 and 4. *Structure of [Cd{Pt(Bdt)(DTBbpy)}$_2$(ClO$_4$)(H$_2$O)](ClO$_4$) (**3**).* Complex **3** was crystallized from CH_2Cl_2/benzene, and the crystallographic study revealed that the complex consists of one trinuclear cation, composed of two platinum moieties and one Cd(II), one H_2O molecule, and two ClO_4^- counteranions, as shown in Figure 2a,b. Selected bond distances and angles are listed in Table 2. The platinum moieties maintain a square-planar Pt center coordinated by two S atoms from the Bdt and two N atoms from the DTBbpy. One of the two platinum moieties designated as **I** is connected to the Cd atom through a Pt → Cd bond together with two S → Cd bonds, while the other moiety (**II**) is bound to the Cd atom by one longer Pt → Cd and one shorter S → Cd bond than those of **I**. The Cd atom is further coordinated by two O atoms from ClO_4^- and H_2O to give a seven-coordinated structure. Here, we note that the observed Pt → Cd bond distances (2.7331(7) and 2.7936(7) Å) are shorter than the sum of the van der Waals radii of Cd and Pt atoms (3.38 Å),[16] indicating apparent dative bond formation. Therefore, this is, to the best of our knowledge, the first example of a Pt → Cd dative bond without strong σ-donor ligands or bridging ligands.[17] Regarding the intramolecular structural influences, the bond distances and angles around the Pt atoms in the platinum moieties are rarely different from **1** (Table 2).[2c] In contrast, the binding of the platinum moieties with the Cd(II) leads to a distortion of the moieties from the ideal planar shape. The dihedral angle (η) between the Bdt (C_6S_2) and the PtS_2N_2 planes listed in Table 2 demonstrates that the η value for **II** is calculated to be 4.73°, which is close to that of the parent **1**, while a larger distortion, 12.34°, is found for **I**, which binds to the Cd atom through two S → Cd bonding interactions. Here we also noted that the presence of the bulky DTB groups leads to a twisted structure, giving rise to a twisted dipole alignment, as shown in Figure 2b, where the opened spaces are filled by ClO_4^- and H_2O molecules. Eventually, the cation in **3** displays chirality (Figure 2c), even though the parent platinum complex, **1**, itself is an achiral molecule. The enantiomers stack alternatively on each other to form a one-dimensional columnar assembly (Figure 2d) in which each cation cancels out its chirality and dipole with the neighboring cation. The two adjacent platinum moieties stack alternatively on each other with mean plane-to-plane distances of 3.466 and 3.432 Å for **I**···**I**′ and **II**···**II**′, respectively. Finally, the other ClO_4^- anion is involved within hydrophobic pockets made by the DTB groups (Figure 2e).

*Structure of [Cd{Pt(Bdt)(C13bpy)}$_3$(H$_2$O)](ClO$_4$)$_2$·CH$_2$Cl$_2$ (**4**).* Figure 3a shows the molecular structure of the cation in **4**, which was crystallized from CH_2Cl_2/*n*-hexane. Complex **4** contains a dicationic, tetranuclear structure, consisting of three platinum moieties and one Cd atom, one H_2O molecule, and two ClO_4^- counteranions. Selected bond distances and angles are summarized in Table 2. The Cd atom lies on the symmetry center, and thus the three platinum moieties are crystallographically equivalent. Similar to **3**, each platinum atom possesses a four-coordinated square-planar geometry, where each two S and N atoms from Bdt and C13bpy, respectively, coordinate to the Pt atom. In addition to the difference in the compositions of **3** and **4**, the most striking structural difference between them is found in the binding modes of the platinum moieties to the Cd atom. In contrast to the dual dative bonds (Pt → Cd and S → Cd) found in **3**, the three platinum moieties in **4** connect to the Cd atom only by S → Cd bonds (2.552(4) Å), which are shorter than all of the three S → Cd bonds found in **3** (Table 2). Along with the significant distortion of the platinum moieties found in **3**, the dihedral angle for **4** is calculated to be only 8.15°. The S_3O-type tetrahedral coordination sphere is formed around the Cd atom by additional coordination of the O atom from H_2O (Figure 3a). As a whole, the cation of complex **4** forms a shuttlecock-shaped structure in which the three platinum moieties align in the same direction so that the dipole moments derived from the moieties are parallel to each other. The view along the Cd−O_{H_2O} bond reveals that the complex forms two cyclic enantiomers, where one molecule has the three platinum

dx.doi.org/10.1021/ic302352k | Inorg. Chem. 2013, 52, 4324−4334

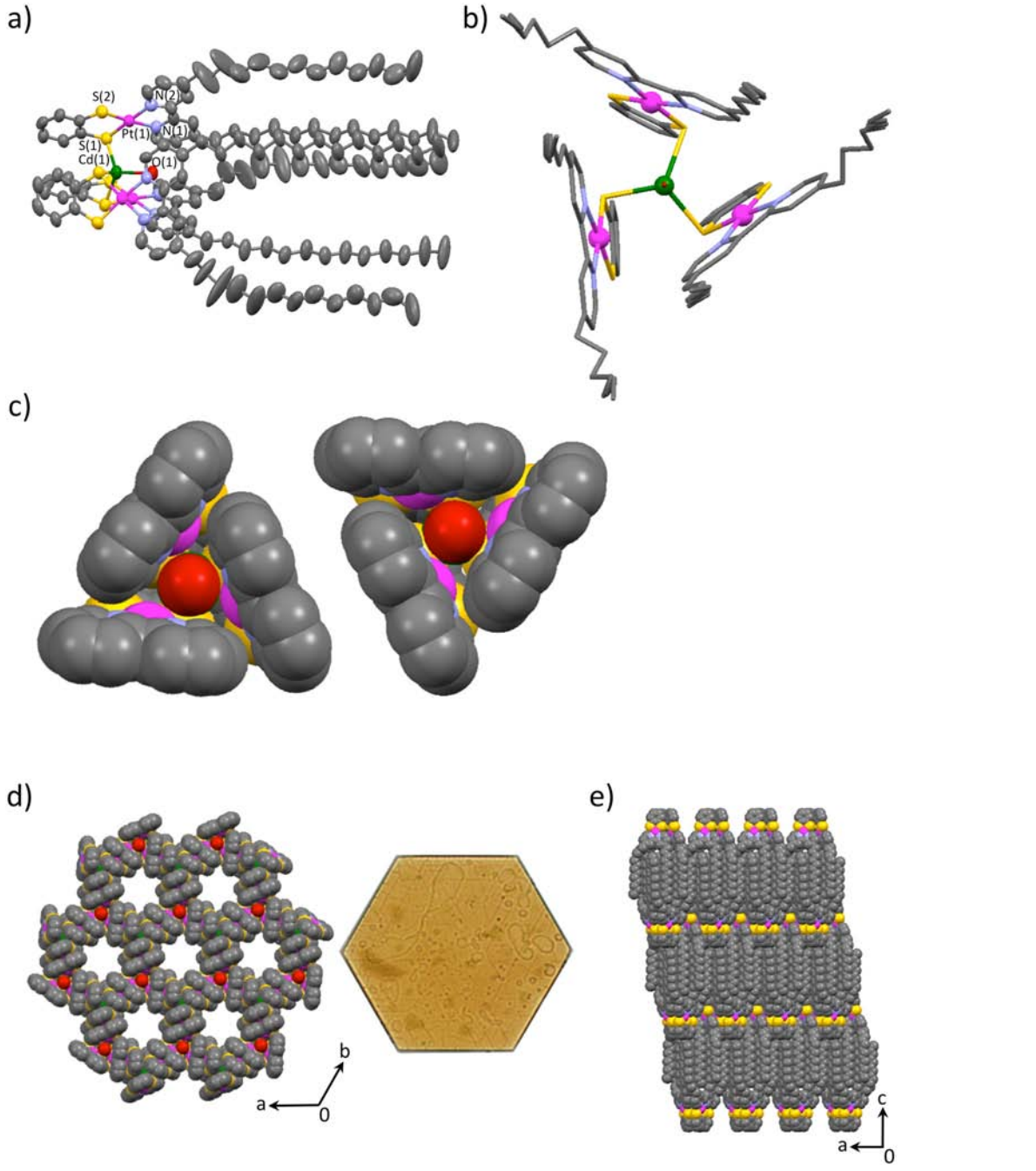

Figure 3. (a) Side (ellipsoid at 50% probability) and (b) top views of the tetranuclear cation in **4** for Cd (green), Pt (magenta), S (yellow), N (blue-purple), O (red), and C (gray). (c) Representation of two forms of the cyclic chiral molecules (clockwise (left) and anticlockwise (right) enantiomers). The tridecyl chains are omitted for clarity. (d) The projection of the two-dimensional honeycomb layer of the cations along the *c*-axis together with a microphotograph of a hexagonal-shaped single crystal of **4**. (e) A projection of the three-dimensional structure of **4** along the *b*-axis.

moieties arranged in a clockwise fashion, and the other molecule has the three platinum moieties arranged in an anticlockwise fashion (Figure 3c). The findings in Figure 3c also allowed us to exclude the possibility of formation of the corresponding tetranuclear structure for **3** and Cd(II) ion because of the steric hindrance of the DTB groups in **3**. In the six tridecyl chains in **4**, of which two chains are crystallographically independent, all methylenes show a *trans* conformation. As Figure 3b shows, each tridecyl chain is closely packed and paired with that of the adjacent platinum moieties to induce a microsegregated structure. Furthermore, each tetranuclear complex stacks with the adjacent molecule by alternating its dipole orientation and chirality to form a two-dimensional honeycomb layer, reflecting the morphology of a single crystal (Figure 3d). The layers are further integrated by means of aliphatic interactions between the tridecyl chains of heterochiral molecules to the direction normal to the honeycomb layer as shown in Figure 3e. As a whole, the complex forms a layer-by-layer structure consisting of two-dimensional layers of the assembled platinum moieties and the aliphatic tridecyl chains. An overview of the molecular and assembled structures of **4** leads to the conclusion that the presence of tridecyl chains drives parallel alignment of each dipole derived from the platinum moieties in the molecule, and

dx.doi.org/10.1021/ic302352k | *Inorg. Chem.* 2013, 52, 4324−4334

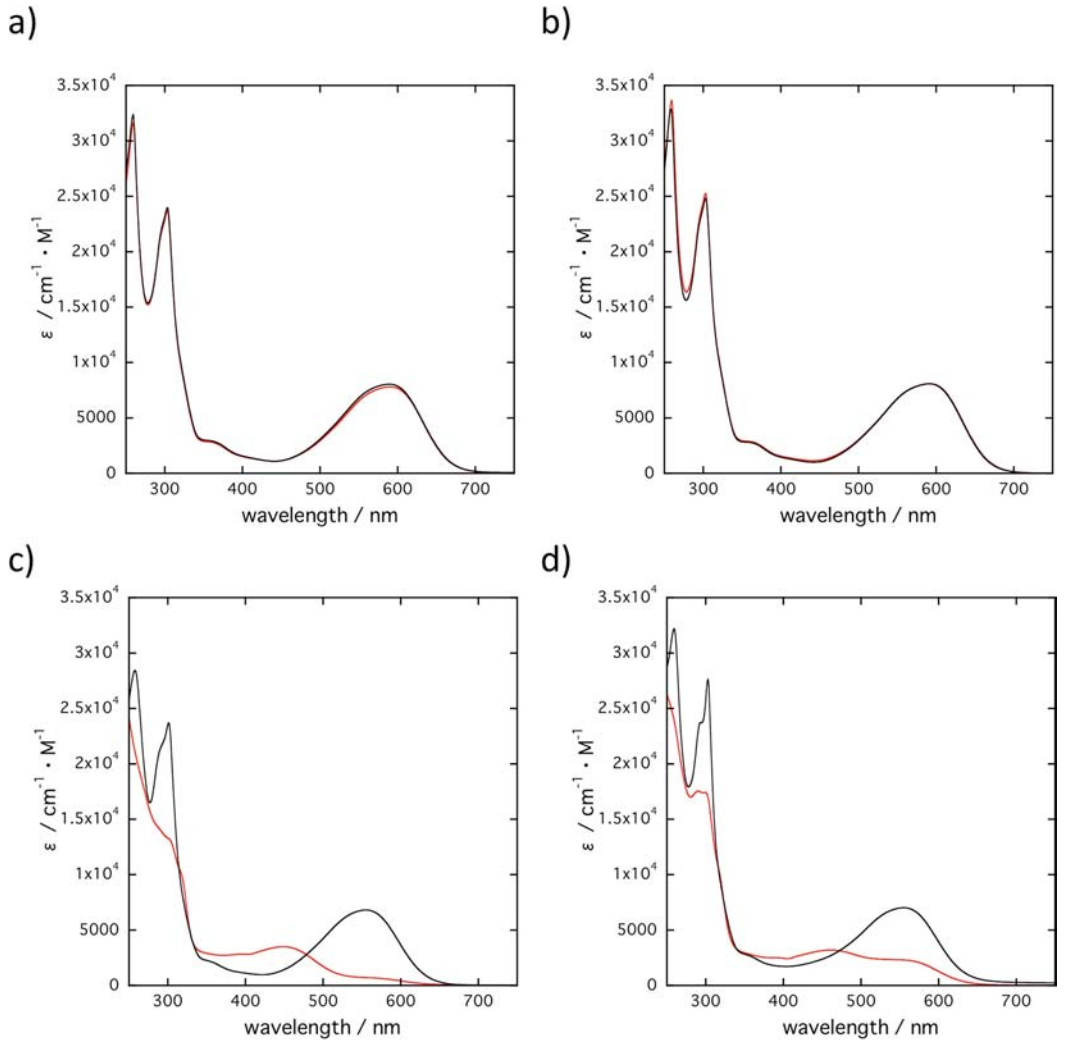

Figure 4. UV−vis absorption spectra of (a) **1** at 1×10^{-4} M (black line) and **3** at 5×10^{-5} M (red line), and (b) **2** at 1×10^{-4} M (black line) and **4** at 3×10^{-5} M (red line) in THF. UV−vis absorption spectra of (c) **1** at 1×10^{-4} M (black line) and **3** at 5×10^{-5} M (red line), and (d) **2** at 1×10^{-4} M (black line) and **4** at 3×10^{-5} M (red line) in CH_2Cl_2.

at the same instant, it leads to antiparallel alignment of the molecules through the intermolecular interactions.

Finally, it is quite important to compare the roles of the dative bonds in the formation of the assembled structures of **3** and **4** with those in the previous examples, for instance, $[PtAg_2(dmbpy)(tdt)(dppm)_2](SbF_6)_2$ and $[PtAu_2(dmbpy)(tdt)(dppm)_2](SbF_6)_2$.[9b,c] In the latter, only one parent Pt moiety bound with the Lewis acids center because of the coordinatively saturated Ag and Au centers, while the presence of the coordinatively unsaturated Cd atom in the present cases resulted in the integration of two (**3**) and three (**4**) parent platinum moieties around the Cd center. Such integrations led not only to structural variations, as shown above, but also to spectrochemical and electrochemical properties with respect to the corresponding parent moieties, as shown below.

Solvent-Dependent Binding Behaviors of the Platinum Moieties with Cd(II) Ion. In contrast to durable dative bonding in the solid state, we found that complexes **3** and **4** demonstrate dynamic behavior in solution. The UV−vis and ^{1}H NMR spectra of **1**−**4** measured in THF and CH_2Cl_2 are shown in Figures 4 and 5, respectively, and the relevant data are listed in Table 3. Complexes **3** and **4** commonly show a blue color in THF and exhibit the most characteristic absorption bands at 590 and 591 nm, respectively, which could be assigned to mixed-metal/ligand-to-ligand charge-transfer (MMLL′CT) bands similar to parents **1** and **2** (Figure 4a,b).[1b,18] In contrast, the absorption spectra of **3** and **4** in CH_2Cl_2 demonstrate bands at 449 and 461 nm, respectively, which are significantly blue-shifted from those of **1** and **2** (Figure 4c,d). Consistent with the electronic absorption spectra, the chemical shifts of **3** and **4** in THF-d_8 coincide with those of **1** and **2** (Figure 5a,b). The spectral similarities of **1**−**4** in THF thus indicate that the platinum moieties and the Cd atom are in dissociating states, suggesting a contribution of coordinative THF molecules.

With regard to the ^{1}H NMR spectra of **3** and **4** in CD_2Cl_2, the significant differences are found in contrast to the behaviors observed in THF-d_8. The chemical shifts of the H_a (Bdt), H_d (bpy), and H_e (bpy) for **3** and **4** commonly shifted downfield compared with those of **1** and **2**, while those of H_b and H_c demonstrate upfield shifts compared with the parent complexes (Figure 5c,d). Contrary to the expectation that aromatic protons in **3** and **4** would shift to lower magnetic field because of the loss of the electron density due to the bound Cd(II), the H_b and H_c assigned to Bdt and bpy, respectively, are shifted to higher magnetic field. This may be due to the shielding effect of the Cd atom with its large atom radius, which becomes larger in

dx.doi.org/10.1021/ic302352k | *Inorg. Chem.* 2013, 52, 4324−4334

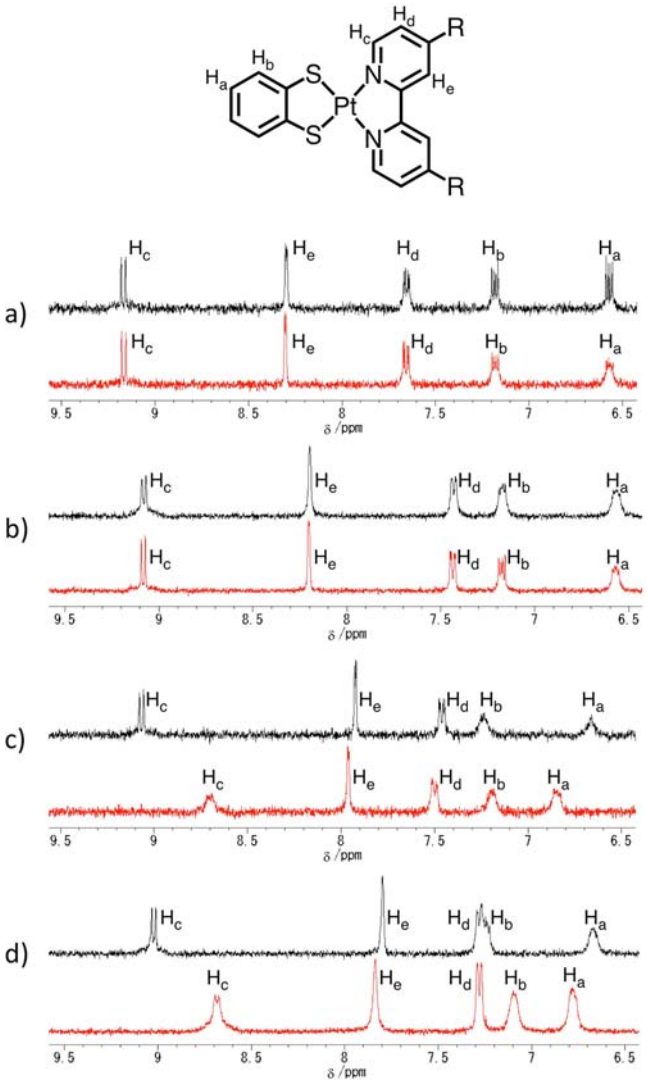

Figure 5. ^{1}H NMR spectra of (a) **1** at 2×10^{-4} M (black line) and **3** at 1×10^{-4} M (red line) and (b) **2** at 3×10^{-4} M (black line) and **4** at 1×10^{-4} M (red line) in THF-d_8. ^{1}H NMR spectra of (c) **1** at 2×10^{-4} M (black line) and **3** at 1×10^{-4} M (red line) and (d) **2** at 3×10^{-4} M (black line) and **4** at 1×10^{-4} M (red line) in CD_2Cl_2.

magnitude than the electron withdrawing effect through the dative bond. Here, we note that the magnitude of the upfield shifts of H_b is smaller than that of H_c. This would be due to lack of direct interaction between the bpys and the Cd atom; thereby, the shielding effect becomes far larger than the electron-withdrawing effect in the case of H_c.[19] In contrast, in the case of H_b, each Bdt binds directly with the Cd atom; therefore, the shielding effect could not respond significantly to the chemical shift as the case of H_c because of the electron-withdrawing effect derived from the S → Cd dative bond formation.[19] In addition, the ^{1}H NMR spectra demonstrate each single signal assignable to H_a-H_e protons, which indicates that each H_a-H_e proton in the platinum moieties is magnetically equivalent in CD_2Cl_2, although the crystallographic analyses indicate the magnetically nonequivalent H_a-H_e protons. It may be reasonable to propose the possible fast association/dissociation equilibria and/or migration of the Cd atom between the S atoms of the platinum moieties takes place through a symmetrical transition state.[19] In contrast to the behaviors in THF, these results indicate that the platinum moieties maintain the dative bonds with Cd(II), which is consistent with the negligible coordination ability of CH_2Cl_2. Therefore, it can be said that the association/dissociation behaviors of the platinum moieties with Cd(II) in **3** and **4** can be modulated by the nature of the solvent molecules.

Table 3. Absorption Spectral Data of 1−4 in THF and in CH_2Cl_2

complex	solvent	concentration/10^{-4} mol·L^{-1}	λ_{abs}/nm (ε/M^{-1}·cm^{-1})[a]
1	THF	1.11	259 (32,400), 295sh (21,800), 303 (24,000)
			356sh (2,960), 589 (8,040)
	CH_2Cl_2	0.971	258 (28,400), 291sh (21,500), 301 (23,700)
			346sh (2,340), 555 (6,810)
2	THF	1.00	258 (32,900), 294sh (22,100), 303 (24,800)
			354sh (2,820), 591 (8,080)
	CH_2Cl_2	0.996	259 (32,200), 293sh (23,700), 303 (27,600)
			347sh (2,900), 555 (7,020)
3	THF	0.497	259 (31,600), 295sh (21,500), 303 (23,700)
			354sh (2,850), 590 (7,810)
	CH_2Cl_2	0.482	305sh (12,900), 319sh (9,690)
			396sh (2,830), 449 (3,500), 553sh (720)
4	THF	0.335	259 (33,700), 295sh (23,000), 303 (25,300)
			357sh (2,900), 591 (8,090)
	CH_2Cl_2	0.345	290 (17,500), 299 (17,400), 317sh (10,500)
			393sh (2,500), 461 (3,200), 558sh (2,290)

[a]Each extinction was calculated based on the Pt moiety.

Luminescence Properties of Lewis-Acid-Bound Complexes. The emission spectra of **1**−**4** in the solid state at 77 K are shown in Figure 6 together with UV−vis spectra measured at room temperature, and the relevant data are listed in Table 4. Complexes **1**−**4** show absorption bands at 450−600 nm, which can be assigned to MMLL′CT bands.[1b,18] The charge-transfer bands of **3** and **4** are blue-shifted in comparison with those of **1** and **2** in solution, indicating the stabilization of the ground states by the dative bonds. Upon excitation of the MMLL′CT bands, complexes **1**−**4** show emission bands at 600−700 nm assigned to emissions from the ^{3}MMLL′CT states.[1b,18] The emission bands of **3** and **4** are also blue-shifted in comparison with those of **1** and **2**, in agreement with the blue-shifted absorption bands. In both absorption and emission spectra, complexes **3** and **4** give rise to broad bands in contrast to the vibronic structured bands for **1** and **2** in the visible region. It was shown that the emission quantum yield (Φ_{em}) of **1** at 77 K is 0.13, while the yield slightly decreases to 0.08 for **3**. In contrast, the emission quantum yield tends to increase to 0.35 for **4** in comparison with 0.26 for **2**. This would have resulted from a suppressed radiationless deactivation process in **4** as a consequence of the effective integration of the platinum moieties around the Cd atom.

Redox Properties of Lewis-Acid-Bound Complexes. The cyclic voltammograms of **1**−**4** measured in CH_2Cl_2 are shown in Figure 7, and the relevant data are listed in Table 5. Complexes **1** and **2** commonly undergo a quasireversible reduction at −1.662 and −1.702 V vs Ag/Ag$^+$, respectively, corresponding to R-bpy-based reduction processes (Figure 7).[8]

dx.doi.org/10.1021/ic302352k | Inorg. Chem. 2013, 52, 4324−4334

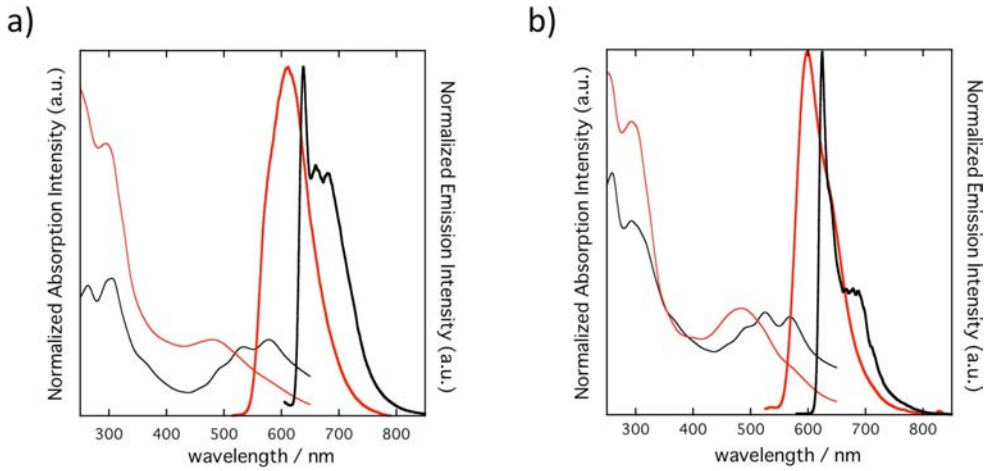

Figure 6. UV−vis absorption (room temperature) and emission spectra (77 K) of (a) **1** (black line) and **3** (red line) and (b) **2** (black line) and **4** (red line) in the solid state.

Table 4. Photoluminescence Properties of 1−4 in the Solid States at 77 K

complex	λ_{abs}/nm (room temperature)	λ_{em}/nm (λ_{ex}/nm) (77 K)	Φ_{em} (77 K)
1	263, 305, 360sh, 490sh, 534, 578	638, 659, 681 (578)	0.13
2	259, 293, 365sh, 490sh, 526, 568	625, 665, 679, 687 (526)	0.26
3	294, 480	646 (480)	0.08
4	293, 483	599 (483)	0.35

In addition, complexes **1** and **2** show oxidation processes on the Pt/Bdt part at E_{pa}^{Ox} = 0.247 and 0.169 V, respectively.[8a]

Complexes **3** and **4** demonstrate a quasireversible reduction at −1.692 and −1.747 V, respectively, similar to those found in **1** and **2**. In contrast to common features of the R-bpy-based reduction processes, complexes **3** and **4** demonstrate multistep irreversible reduction peaks around −1.0 to −1.5 V, dissimilar from **1** and **2**. The durable dative bonds in CH_2Cl_2, proved by the above-mentioned spectroscopic studies, lead us to tentatively assign these new reduction processes as electrochemical reductions on the Pt(II) center. With regard to the oxidation processes of **3** and **4**, complex **3** exhibits two irreversible anodic peaks at 0.438 and 0.629 V, while complex **4** shows three irreversible anodic peaks at 0.199, 0.399, and 0.584 V (Figure 7). It is noteworthy that the numbers of multistep oxidation processes for **3** and **4** correspond to the numbers of platinum moieties. Thus, these results suggest that the platinum moieties in **3** and **4** have electronic interactions through the Cd atom, plausibly leading to the formation of one and two mixed-valent species during the oxidation processes. Furthermore, significant positive shifts of the first oxidation potentials are observed for **3** and **4** compared with those for **1** and **2**, indicating that the redox properties of the platinum moieties could be modulated not only by the alkyl groups substituted on the bpy but also by the bindings of the Lewis acid.

■ CONCLUSIONS

The present study has shown a new approach to assembling functional moieties, [Pt(Bdt)(R-bpy)], through dative bond interaction with Cd(II). This study proved that complexes **1** and **2** commonly act as a metalloligand toward Cd(II) to form trinuclear or tetranuclear complexes **3** and **4**, respectively, where remarkable alkyl group dependence was observed. Through their binding interaction with Cd(II), significant blue shifts in both absorption and emission spectra were

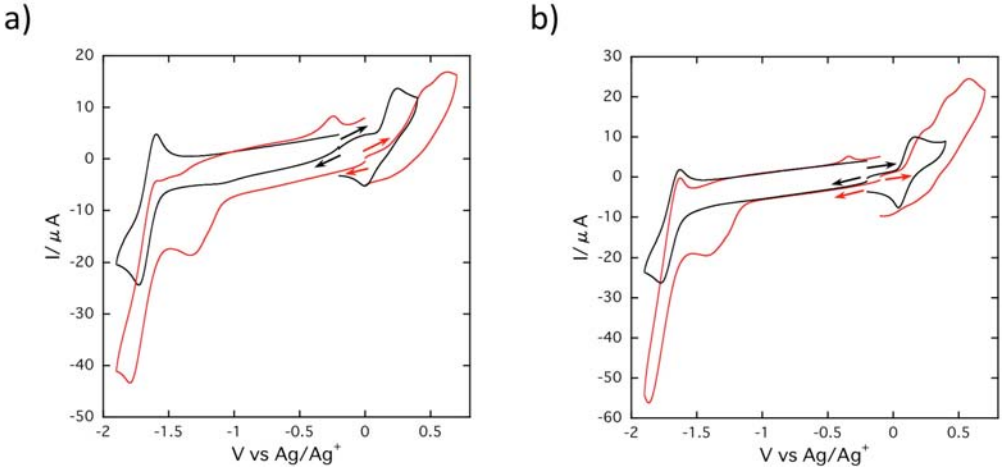

Figure 7. Cyclic voltammograms of (a) **1** (black line) and **3** (red line) and (b) **2** (black line) and **4** (red line) in CH_2Cl_2 in the presence of 0.1 M *n*-Bu_4NClO_4 under Ar at 100 mV/s.

dx.doi.org/10.1021/ic302352k | *Inorg. Chem.* 2013, 52, 4324−4334

Table 5. Electrochemical Data of 1−4 in CH_2Cl_2

complex	$E_{1/2}^{Red}$	E_{pc}^{Red}	E_{pa}^{Red}	E_{pc}^{Ox}	E_{pa}^{Ox}	E_{pa}^{Ox}	E_{pa}^{Ox}
1	−1.662			−0.003	0.247		
2	−1.702			0.040	0.169		
3	−1.692	−1.336[a]	−0.238[a]		0.438[a]	0.629[a]	
4	−1.747	−1.429[a]	−0.339[a]		0.199[a]	0.399[a]	0.584[a]

[a]Irreversible wave.

observed. The present study also revealed for the first time that integration of the moieties also leads enrichment of the redox properties, where multistep oxidation processes are observed corresponding to the number of platinum moieties. These results represent the electronic communications between the platinum moieties through the Cd atom. We also found that modification of the alkyl parts on the R-bpy gives rise to a variation in the assembled structures; thereby, structural, spectroscopic, and redox properties can be varied. It is expected that further physicochemical properties of [Pt(Bdt)(R-bpy)] can be controlled by connection with specific Lewis acids.

■ ASSOCIATED CONTENT

Ⓢ Supporting Information

X-ray crystallographic data for complexes **3** and **4** in CIF format. Differential pulse voltammograms, IR spectra, NMR spectra in DMF-d_7 and $CDCl_3$, and emission spectra of **1**−**4** in CH_2Cl_2 at 77 K. This material is available free of charge via the Internet at http://pubs.acs.org.

■ AUTHOR INFORMATION

Corresponding Author

*E-mail: chang@sci.hokudai.ac.jp.

Notes

The authors declare no competing financial interest.

■ ACKNOWLEDGMENTS

This work was financially supported in part by a Grant-in-Aid for Scientific Research for Priority Area "Coordination Programming" (Area No. 2107) and the project for the Effective Utilization of Elements from the Ministry of Education, Culture, Sports, Science, and Technology, Japan.

■ REFERENCES

(1) (a) Williams, J. A. G. *Top. Curr. Chem.* **2007**, *281*, 205. (b) Hissler, M.; McGarrah, J. E.; Connick, W. B.; Geiger, D. K.; Cummings, S. D.; Eisenberg, R. *Coord. Chem. Rev.* **2000**, *208*, 115−137. (c) Houlding, V. H.; Miskowski, V. M. *Coord. Chem. Rev.* **1991**, *111*, 145−152.

(2) (a) Sakai, K.; Ozawa, H. *Coord. Chem. Rev.* **2007**, *251*, 2753−2766. (b) Zhang, J.; Du, P.; Schneider, J.; Jarosz, P.; Eisenberg, R. *J. Am. Chem. Soc.* **2007**, *129*, 7726−7727. (c) Lazarides, T.; McCormick, T. M.; Wilson, K. C.; Lee, S.; McCamant, D. W.; Eisenberg, R. *J. Am. Chem. Soc.* **2011**, *133*, 350−364. (d) Du, P.; Schneider, J.; Li, F.; Zhao, W.; Patel, U.; Castellano, F. N.; Eisenberg, R. *J. Am. Chem. Soc.* **2008**, *130*, 5056−5058.

(3) (a) Connick, W. B.; Henling, L. M.; Marsh, R. E.; Gray, H. B. *Inorg. Chem.* **1996**, *35*, 6261−6265. (b) Wong, K. M.-C.; Yam, V. W.-W. *Acc. Chem. Res.* **2011**, *44*, 424−434. (c) Po, C.; Tam, A. Y.-Y.; Wong, K. M.-C.; Yam, V. W.-W. *J. Am. Chem. Soc.* **2011**, *133*, 12136−12143. (d) Sun, Y.; Ye, K.; Zhang, H.; Zhang, J.; Zhao, L.; Li, B.; Yang, G.; Yang, B.; Wang, Y.; Lai, S.-W.; Che, C.-M. *Angew. Chem., Int. Ed.* **2006**, *45*, 5610−5613.

(4) Cocker, T. M.; Bachman, R. E. *Mol. Cryst. Liq. Cryst.* **2004**, *408*, 1−19.

(5) Janzen, D. E.; Patel, K.; VanDerveer, D. G.; Grant, G. J. *J. Chem. Crystallogr.* **2006**, *36*, 83−91.

(6) Aakeröy, C. B.; Beatty, A. M.; Leinen, D. S. *Angew. Chem., Int. Ed.* **1999**, *38*, 1815−1819.

(7) (a) Lai, S.-W.; Chan, M. C.-W.; Cheung, T.-C.; Peng, S.-M.; Che, C.-M. *Inorg. Chem.* **1999**, *38*, 4046−4055. (b) Yam, V. W.-W. *Acc. Chem. Res.* **2002**, *35*, 555−563. (c) Wong, K. M.-C.; Yam, V. W.-W. *Coord. Chem. Rev.* **2007**, *251*, 2477−2488. (d) Kui, S. C. F.; Chui, S. S.-Y.; Che, C.-M.; Zhu, N. *J. Am. Chem. Soc.* **2006**, *128*, 8297−8309. (e) Kui, S. C. F.; Sham, I. H.T.; Cheung, C. C. C.; Ma, C.-W.; Yan, B.; Zhu, N.; Che, C.-M.; Fu, W.-F. *Chem.—Eur. J.* **2007**, *13*, 417−435.

(8) (a) Chang, H.-C.; Komasaka, K.; Kishida, K.; Shiozaki, T.; Ohmori, T.; Matsumoto, T.; Kobayashi, A.; Kato, M.; Kitagawa, S. *Inorg. Chem.* **2011**, *50*, 4279−4288. (b) Chang, H.-C.; Shiozaki, T.; Kamata, A.; Kishida, K.; Ohmori, T.; Kiriya, D.; Yamauchi, T.; Furukawa, H.; Kitagawa, S. *J. Mater. Chem.* **2007**, *17*, 4136−4138.

(9) (a) Yamaguchi, T.; Yamazaki, F.; Ito, T. *J. Am. Chem. Soc.* **1999**, *121*, 7405−7406. (b) Chen, Y.-D.; Qin, Y.-H.; Zhang, L.-Y.; Shi, L.-X.; Chen, Z.-N. *Inorg. Chem.* **2004**, *43*, 1197−1205. (c) Chen, Y.-D.; Zhang, L.-Y.; Shi, L.-X.; Chen, Z.-N. *Inorg. Chem.* **2004**, *43*, 7493−7501. (d) Fuertes, S.; Woodall, C. H.; Raithby, P. R.; Sicilia, V. *Organometallics* **2012**, *31*, 4228−4240. (e) Arsenault, G. J.; Anderson, C. M.; Puddephatt, R. J. *Organometallics* **1988**, *7*, 2094−2097. (f) Moret, M. E. *Top. Organomet. Chem.* **2011**, *35*, 157−184.

(10) (a) Parr, R. G.; Pearson, R. G. *J. Am. Chem. Soc.* **1983**, *105*, 7512−7516. (b) Pearson, R. G. *J. Am. Chem. Soc.* **1963**, *85*, 3533−3539.

(11) Kiriya, D.; Chang, H.-C.; Kamata, A.; Kitagawa, S. *Dalton Trans.* **2006**, 1377−1382.

(12) Burla, M. C.; Caliandro, R.; Camalli, M.; Carrozzini, B.; Cascarano, G. L.; De Caro, L.; Giacovazzo, C.; Polidori, G.; Spagna, R. *J. Appl. Crystallogr.* **2005**, *38*, 381−388.

(13) Beurskens, P. T.; Admiraal, G.; Beurskens, G.; de Gelder, R.; Garcia-Granda, S.; Gould, R. O.; Israel, R.; Smits, J. M. M. *DIRDIF-99*; University of Nijmegen: Nijmegen, The Netherlands, 1999.

(14) *CrystalStructure 3.8.2, Crystal Structure Analysis Package*; Rigaku and Rigaku/MSC: The Woodlands, TX, 2000−2006.

(15) Sheldrick, G. *SHELX-97, Program for Crystal Structure Solution and the Refinement of Crystal Structures*; Institüt für Anorganische Chemie der Universität Göttingen: Göttingen, Germany, 1997.

(16) Bondi, A. *J. Phys. Chem.* **1964**, *68*, 441−451.

(17) (a) Charmant, J. P. H.; Falvello, L. R.; Forniés, J.; Gómez, J.; Lalinde, E.; Moreno, M. T.; Orpen, A. G.; Rueda, A. *Chem. Commun.* **1999**, 2045−2046. (b) Forniés, J.; Gómez, J.; Lalinde, E.; Moreno, M. T. *Inorg. Chem.* **2001**, *40*, 5415−5419. (c) Chen, W.; Liu, F.; Nishioka, T.; Matsumoto, K. *Eur. J. Inorg. Chem.* **2003**, 4234−4243. (d) Forniés, J.; Ibáñez, S.; Martín, A. *Organometallics* **2004**, *23*, 3963−3975. (e) Berenguer, J. R.; Gil, B.; Fernández, J.; Forniés, J.; Lalinde, E. *Inorg. Chem.* **2009**, *48*, 5250−5262. (f) Berenguer, J. R.; Fernández, J.; Gil, B.; Lalinde, E.; Sánchez, S. *Inorg. Chem.* **2010**, *49*, 4232−4244.

(18) (a) Paw, W.; Cummings, S. D.; Mansour, M. A.; Cennick, W. B.; Geiger, D. K.; Eisenberg, R. *Coord. Chem. Rev.* **1998**, *171*, 125−150. (b) Sakamoto, R.; Murata, M.; Kume, S.; Sampei, H.; Sugimoto, M.; Nishihara, H. *Chem. Commun.* **2005**, 1215−1217. (c) Islam, A.; Sugihara, H.; Hara, K.; Singh, L. P.; Katoh, R.; Yanagida, M.; Takahashi, Y.; Murata, S.; Arakawa, H. *Inorg. Chem.* **2001**, *40*, 5371−5380. (d) Connick, W. B.; Geiger, D.; Eisenberg, R. *Inorg. Chem.* **1999**, *38*, 3264−3265. (e) Cummings, S. D.; Eisenberg, R. *J. Am. Chem. Soc.* **1996**, *118*, 1949−1960. (f) Vanhelmont, F. W. M.; Johnson, R. C.;

Hupp, J. T. *Inorg. Chem.* **2000**, *39*, 1814−1816. (g) Makedonas, C.; Mitsopoulou, C. A.; Lahoz, F. J.; Balana, A. I. *Inorg. Chem.* **2003**, *42*, 8853−8865. (h) Makedonas, C.; Mitsopoulou, C. A. *Spectrochim. Acta, Part A* **2006**, *64*, 918−930. (i) Ghosh, P.; Begum, A.; Herebian, D.; Bothe, E.; Wieghardt, K. *Angew. Chem., Int. Ed.* **2003**, *42*, 563−567. (j) Makedonas, C.; Mitsopoulpou, C. A. *Inorg. Chim. Acta* **2007**, *360*, 3997−4009. (k) Zuleta, J. A.; Bevilaacqua, J. M.; Proserpio, D. M.; Harvey, P. D.; Eisenberg, R. *Inorg. Chem.* **1992**, *31*, 2396−2404. (l) Sakamoto, R.; Kume, S.; Sugimoto, M.; Nishihara, H. *Chem.—Eur. J.* **2009**, *15*, 1429−1439.

(19) Juliá, F.; Jones, P. G.; González-Herrero, P. *Inorg. Chem.* **2012**, *51*, 5037−5049.